



ELSEVIER

Available online at www.sciencedirect.com

SCIENCE @ DIRECT®

Nuclear Instruments and Methods in Physics Research A 521 (2004) 407–415

**NUCLEAR
INSTRUMENTS
& METHODS
IN PHYSICS
RESEARCH**
Section A

www.elsevier.com/locate/nima

Low-temperature study of 35 photomultiplier tubes for the ZEPLIN III experiment

H.M. Araújo^{a,*}, A. Bewick^a, D. Davidge^a, J. Dawson^a, T. Ferbel^{a,1}, A.S. Howard^a,
W.G. Jones^a, M. Joshi^a, V. Lebedenko^{a,2}, I. Liubarsky^a, J.J. Quenby^a,
T.J. Sumner^a, F. Neves^b

^a *Astrophysics Group, Blackett Laboratory, Imperial College London, London SW7 2BW, UK*

^b *LIP-Coimbra, University of Coimbra, Portugal*

Received 10 July 2003; received in revised form 10 October 2003; accepted 19 October 2003

Abstract

A set of 35 photomultiplier tubes (ETL D730/9829Q), intended for use in the ZEPLIN III Dark Matter detector, was tested from room temperature down to -100°C , with the aim of confirming their suitability for detecting xenon scintillation light at 175 nm while immersed in the cryogenic liquid. A general improvement of both gain and quantum efficiency at the xenon scintillation wavelength was observed with cooling, the best combined effect being 40%, while little change was noted in the timing properties and dark current. Saturation of response due to accumulation of charge in the resistive bialkali photocathodes was seen at an average photocurrent of 10^8 photoelectrons/s for the device with best quantum efficiency, whereas an order of magnitude higher current was required to saturate the least sensitive one. Variations in photocathode thickness from tube to tube could account for this behaviour, as well as the fact that the quantum efficiency improves the most for devices with poorest efficiency at room temperature.

© 2003 Elsevier B.V. All rights reserved.

PACS: 85.60.Ha; 29.40.Mc

Keywords: Photomultiplier tubes; Cooled photomultipliers; Liquid xenon

1. Introduction

Photomultiplier tubes (PMTs) are often the preferred photon detector for experiments involving scintillation and/or electroluminescence in

liquid xenon and other condensed noble gases. This is the case for experiments being run or under construction by the Boulby Dark Matter Collaboration. In particular, the ZEPLIN III detector for Weakly Interacting Massive Particles (WIMPs) will employ 31 2-in. PMTs to detect the vacuum ultraviolet (VUV) scintillation from liquid and gaseous xenon [1].

In liquid xenon systems, PMTs are usually required to have a high quantum efficiency (QE $\sim 30\%$), fast response (~ 1 ns), low dark

*Corresponding author.

E-mail address: h.araujo@imperial.ac.uk (H.M. Araújo).

¹Current address: Department of Physics, University of Rochester, NY 14627, USA.

²On leave from Institute of Theoretical and Experimental Physics, Moscow, Russia.

current, and the ability to operate at temperatures of -100°C or below. Photomultipliers with bi-alkali photocathodes are known to exhibit significant loss of sensitivity at such low temperatures because of the rapidly increasing photocathode resistivity and the consequent charging brought about by photoelectron emission (see [2–5] and references therein). We describe studies of the low-temperature response of 35 PMTs (ETL D730³ [6]) for use in the ZEPLIN III detector. Their photocathodes have been specially provided with six metal strips, or ‘fingers’, disposed radially, in order to decrease the average resistance and extend the operating temperature range. The D730 PMTs are otherwise very similar to the parent model ETL 9829Q.

Previous tests investigating the low-temperature behaviour of PMTs with bi-alkali photocathodes revealed that some tubes show significant increase in QE between room temperature and -100°C when illuminated at xenon scintillation wavelengths ($\approx 175\text{ nm}$) before saturation sets in [4,5]. Increases by factors of up to 2.5 were observed for some PMTs, while others, tested in the same setup, exhibited little change. The QE is often enhanced in the blue part of the spectrum upon cooling due to a decrease in lattice scattering. However, the significant change observed in the VUV for some PMTs cannot be explained solely by this.

In light of these findings, it seemed wise to calibrate the QE at low temperature prior to assembling ZEPLIN III. In addition, the study of 35 PMTs, which had several specific selection criteria required of the manufacturer, provided a degree of statistical significance to their characterisation that could reveal the origin of this behaviour. This issue is addressed by the first set of tests described in this paper, in which xenon scintillation is used as the light source.

Another key aim of this work was to confirm the cold operation of the PMTs at the light intensities expected in ZEPLIN III, especially during calibration of the instrument using external radioactive sources. Radioactivity from the PMTs themselves is expected to deposit about 1 MeV/s in the active

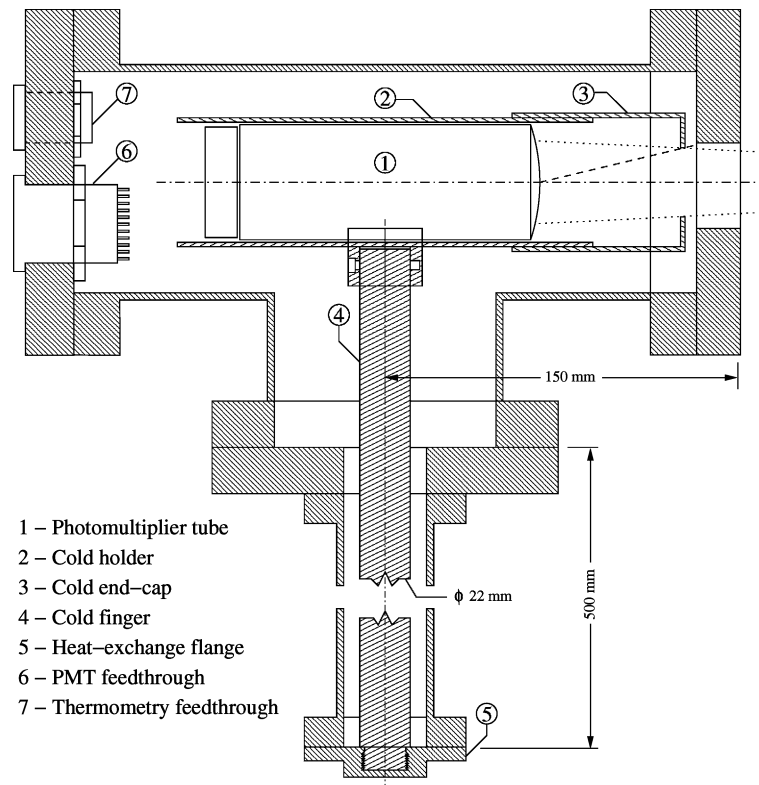
region, which should be the biggest source of background for operation underground. Electroluminescence converts the corresponding ionisation charge into large numbers of VUV photons, which we estimate to be $<10^6/\text{s/PMT}$. This is comparable to the average photon rate produced by the xenon scintillation cell used in these tests, and it should not cause appreciable charging effects. However, operation at the surface and calibration with γ -rays and neutrons will produce much higher count rates, which can overwhelm the PMTs. A green LED was used for those tests requiring higher photon rates.

2. Experimental procedure

The VUV tests were carried out in a special purpose vacuum cryostat, with the PMT illuminated by a gaseous xenon scintillation cell. The cryostat, shown in Fig. 1, offers several advantages over tests relying on convection cooling. In particular, it is easy to thermally decouple the light source from the cold elements, the gas intervening in the optical path is not a concern, and the set-up requires little attention during cooling. The cryostat consists of a vacuum vessel and an inner cylindrical copper shell, which houses the tube. A 70-cm long copper rod (the cold finger) connects this holder to a sealed flange at the bottom of the set-up, which is immersed in liquid nitrogen to provide the cooling. The cryostat is evacuated to $<10^{-3}\text{ mbar}$ by sorption pumps (the system is oil-free). Typically, the PMT reaches -100°C two hours after the bottom flange is immersed in liquid nitrogen.

The temperature is measured with a thermocouple pressed against the side of the tube very near the quartz window. Apart from the holder, the main thermal inputs to the PMT are radiation from the warm surroundings and the wiring to the feedthrough connectors (the voltage divider is located outside the cryostat). The heat introduced through the wires is small compared to that carried away by the holder, and from the latter to the cold finger. As the envelope is made of thin glass, the temperature along the PMT envelope should be relatively uniform. We estimate that the tempera-

³The D730 is a 2-inch photomultiplier based on model ETL 9829Q (quartz window, bi-alkali photocathode, 12 linear-focused CuBe dynodes).



- 1 – Photomultiplier tube
- 2 – Cold holder
- 3 – Cold end-cap
- 4 – Cold finger
- 5 – Heat-exchange flange
- 6 – PMT feedthrough
- 7 – Thermometry feedthrough

Fig. 1. Vacuum cryostat. The field-of-view from the VUV source is indicated by the dotted line. The dashed line represents the field-of-view defined by the cold stop.

ture difference between opposite ends of the PMT is no more than a couple of degrees.

Significant warming of the PMT window by radiation from the warm surroundings is prevented by the end-cap shown in the figure. The 30 mm cold-stop, which defines the aperture for VUV radiation, illuminates a photocathode area 36 mm in diameter (60% of the sensitive area). The resulting 25° field-of-view for ambient temperature reduces the thermal loading considerably. The temperature difference between the centre of the window and the envelope can be estimated for a disk of radius r and thickness h , illuminated with a power p per unit area: $\Delta T = pr^2/4\kappa h \approx 1^\circ\text{C}$, where κ is the thermal conductivity ($\sim 1 \text{ W/K/m}$ for quartz at -100°C).

The scintillation cell (not shown) is attached to the right of the cryostat. It is made from stainless-steel tubing, sealed with a 3-mm thick MgF_2

window. After cleaning with organic solvents and baking, it is pumped out to a few times 10^{-10} mbar, and then filled with ultra-pure xenon at 3.3 bar. An ^{241}Am α source mounted near the rear flange produces scintillation photons at approximately 175 nm. At this pressure, the range for α particles is about 5 mm. The scintillation yield is not observed to change with xenon pressure or temperature near ambient conditions. The cell is completely decoupled thermally from the cold PMT holder, and remains at room temperature throughout the test.

Despite its initial purity, the xenon gas becomes progressively contaminated by causes such as outgassing from the epoxy compound used to glue the window. As a consequence, the light yield decreases slowly with time. This effect was monitored through periodic measurements with the same PMT. It was found that the scintillation

intensity decreased essentially linearly with time to about one half of its initial value during the test period, as shown in Fig. 2.

The PMT is biased positively using a voltage divider designed to enhance pulse linearity (5R-R-R-...-R-2R-2.5R-3.6R-5.7R). A voltage $V_{k-a} = 2200$ V ($V_{k-d_1} = 410$ V) sets a gain of approximately 10^7 . The divider network is located outside the cryostat at room temperature. The anode signal is amplified and shaped, and the pulse height recorded with a multichannel analyser (MCA). Fig. 3 shows a typical spectrum. The single-electron response (SER) is monitored by allowing a controllable amount of ambient light to leak into the system. The VUV response is measured by fitting a Gaussian curve to the main peak. The number of photoelectrons (phe) is calculated from the ratio of this VUV signal to the SER peak. A small systematic error, of a fraction of 1 phe, is inherent in this procedure due to photoelectron statistics. However, this is difficult to correct due to the broadening of the pulse height distribution by the intrinsic spread in α -particle energies from the source.

The average number of incident photons per scintillation pulse (of order 50) is calibrated using the mean of the nominal quantum efficiencies at

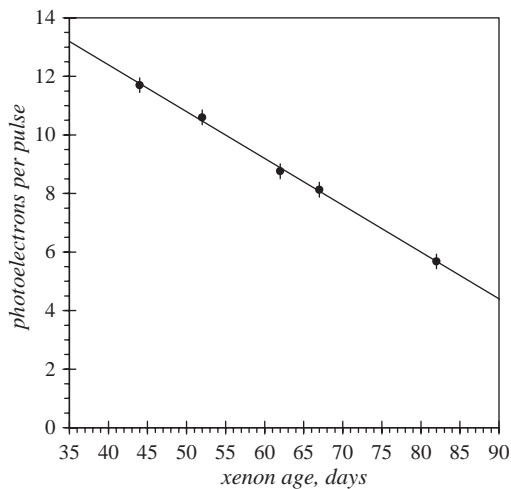


Fig. 2. Mean number of photoelectrons per α particle obtained with the same PMT as a function of time. The data are well fitted by a linear dependence with a slope of $-(0.163 \pm 0.009)$ phe/day.

175 nm provided by ETL for each PMT, together with the established decrease in signal of 0.88 photons/day. The efficiency is then recalculated for each tube. Fig. 4 indicates the relative difference between the new and nominal values. The figure confirms that the decrease in light yield over time is well parameterised. The width of the

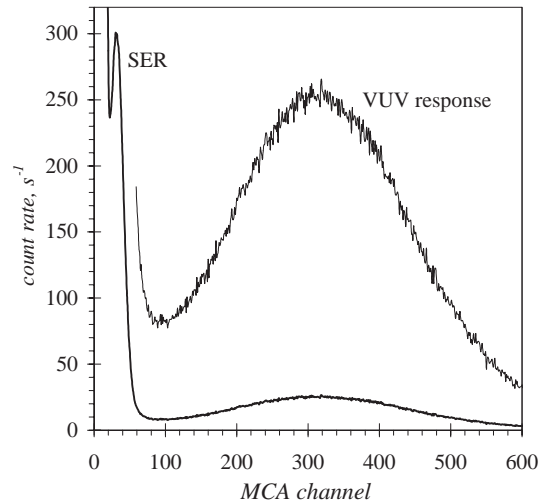


Fig. 3. A typical pulse height spectrum, showing the VUV signal (also shown on an enlarged scale) and the stimulated single-electron response (SER).

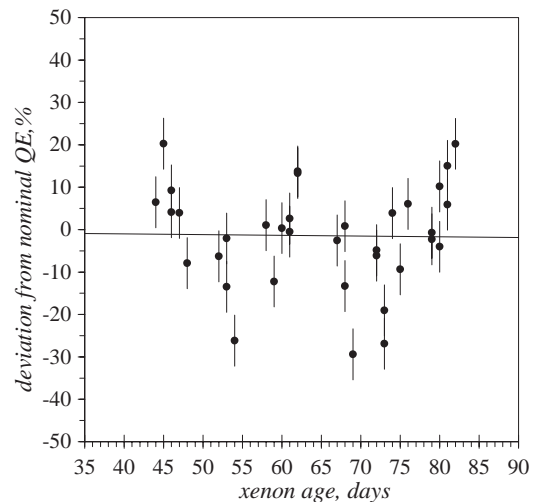


Fig. 4. QE re-calibration at 175 nm for all PMTs, corrected for xenon contamination, plotted as a function of time elapsed from filling of the cell with pure xenon.

distribution is consistent with the accuracy quoted by the manufacturer for their calibration. It should be noted that this uncertainty does not take into account systematic errors inherent in the ETL calibration, and those due to differences between the calibration waveband and the scintillation spectrum of gaseous xenon.

For saturation tests, the xenon cell was replaced by a green LED operated in pulsed mode. The LED illuminated an area of the photocathode 42 mm in diameter, producing ~ 5000 phe per pulse (~ 1 μ s wide). The photon flux was varied by changing the pulse repetition rate. The photocurrent was calibrated against the SER as described previously.

3. Results

3.1. VUV measurements

The temperature dependence of the response to xenon scintillation is shown in Fig. 5 for the PMT with lowest QE at 175 nm (18%). Measurements of this tube were taken during both cooling and re-warming of the cryostat. The signal increased

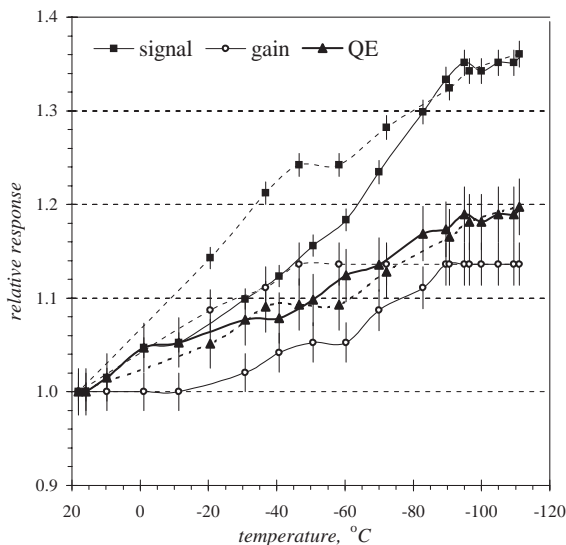


Fig. 5. Cooling test with 175 nm xenon scintillation light. Continuous lines represent the response during cooling, dotted lines refer to the subsequent warming period.

approximately 35% between room temperature and -100°C , recovering the original gain and sensitivity after warming up. It is apparent that the behaviour observed during cooling is not exactly retraced during warming. This hysteresis effect can be traced to gain (SER) variations, and is probably due to the poor thermal conductance between the dynode structures and the glass envelope. The photocathode thermalises more quickly, so the QE curves overlap. The quantum efficiency at 175 nm increases linearly by 20% between room temperature and -100°C .

Similar behaviour was observed in the majority of the tests: an increase in response was seen for all but 3 tubes. Of these, two showed an increase in QE despite small decreases in overall response with cooling. Only one exhibited a decrease in QE as well as gain. The response of some PMTs was observed to peak before -100°C , and then to decrease by this temperature. This effect was attributed to changes in gain rather than quantum efficiency. Several tubes were checked after warm up, and observed to recover the original room temperature characteristics to within about 5%.

Overall, the sample showed a wide variation in temperature-induced changes in gain, ranging from -5% to $+25\%$. This may be partly explained by the fact that the dynode chain may not have fully thermalised with the tube envelope, even though Fig. 5 suggests that this effect is not severe near -100°C , which is relatively close to the minimum temperature reached in this cryostat (-120°C). Also, as we have stated, the gain of some tubes peaks above -100°C whilst others show a monotonic increase down to at least that temperature. Nevertheless, all but 3 PMTs showed a net increase in gain with cooling, suggesting that the CuBe dynodes have a negative temperature coefficient for secondary electron emission down to a temperature of the order of -100°C .

Cooling affects the QE at 175 nm of all PMTs in the sample. Fig. 6 shows the relative change observed between room temperature and -100°C , plotted as a function of the QE measured by us at room temperature. It is clear that tubes with poorest QE tend to improve most with cooling ($+20\%$), while the best ones show only a moderate increase ($+5\%$). However, this effect

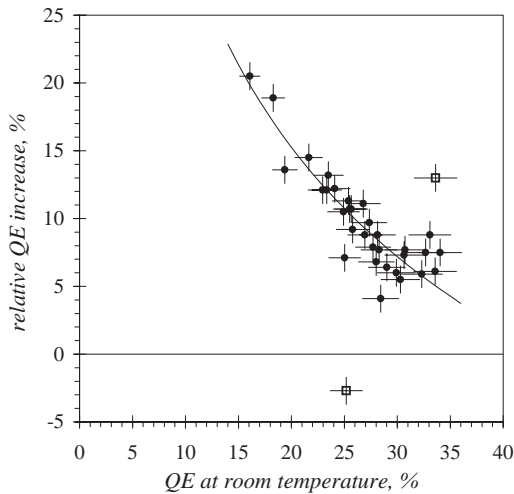


Fig. 6. Relative change between room temperature and -100°C of the quantum efficiency at 175 nm as a function of the initial room temperature value.

does not dominate over the initial QE selection. The tubes represented by the empty squares were tested twice, and the results were confirmed within errors. The line shown in the figure is a power-law fit to the data (excluding those two points), which is motivated by a simple model described in Section 4.

3.2. Measurements with green LED

These measurements were intended mainly to establish the saturation photocurrent, and its dependence on temperature and applied voltage. Three tubes were tested: two D730—those with lowest and highest QE out of the 35 (18.3% and 32.3%, denoted as #1 and #2, respectively)—and one ETL 9829QA (23%), which is the parent model for the D730 (without the photocathode fingers).

The response to the pulsed green LED showed a 9% decrease in QE between room temperature and -100°C . This behaviour, which reflects the shift of the sensitivity curve towards shorter wavelengths, is common in alkali photocathodes, and was not explored further.

The photocathode saturation curves, shown in Fig. 7, were measured in the following way. Upon

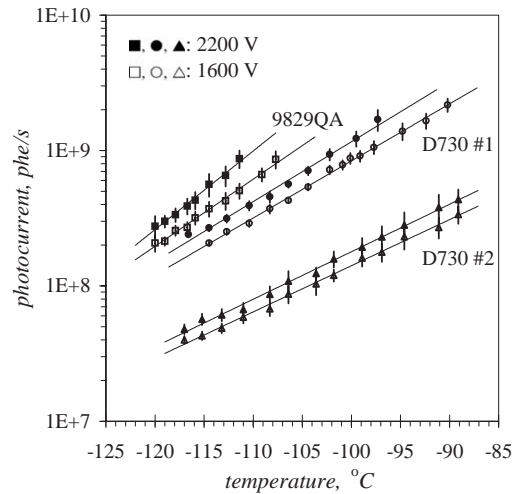


Fig. 7. Temperature dependence of the average photocurrent required to saturate the photocathode response to 50% of its value at low light intensities, for D730 and 9829QA tubes operating at two different voltages.

reaching its equilibrium temperature at -120°C , the cryostat is allowed to warm up slowly. The repetition rate of the LED is then increased until the signal amplitude decreases by 50% relative to its original value at low rate. The procedure is repeated every 1–2 degrees for applied voltages of 1600 V ($V_{k-d_1} = 300$ V) and 2200 V ($V_{k-d_1} = 410$ V) until, eventually, pile up of the pulses sets on before saturation can be observed. The saturated signal is relatively stable during the measurement and the response recovers fully once the light intensity is decreased. A recovery time constant of a few seconds is observed for the D730 tubes, and of a few tens of seconds for the 9829Q.

Fig. 7 reveals an exponential variation of the saturation current with temperature, a trend due to the well-known exponential increase in resistivity of alkali photocathodes upon cooling. The data also indicate that larger average photocurrents can be tolerated with higher bias voltages, as more charge must accumulate to counteract the extraction field. It is less clear why the D730 photocathodes, which have metal fingers, saturate more easily than the 9829Q tested, although they recover more quickly than the latter. It is also worth stressing that the tube with lowest QE

(D730 #1) saturates at a higher average current than the best one (D730 #2).

3.3. Timing response and dark current

Time constant analysis of the prompt liquid-xenon scintillation signal could be a valuable complementary technique in ZEPLIN III to discriminate between different interacting particle species. Scintillation decay times in the range of 3 to 45 ns can be observed in liquid xenon depending on the electric field strength and the type of interaction (electron or nuclear recoil). A degradation of the timing performance has been observed at high VUV photon rates for an ETL 9829Q PMT in our double-phase xenon prototype detector (a description of this system can be found in [7]). This manifested itself in a noticeable increase in rise time at -100°C . The timing performance of the ZEPLIN III tubes does not change significantly at low temperatures for photon rates too low to cause saturation. The rise and decay times for single photoelectrons (≈ 3 ns) remain unchanged between room temperature and -100°C , as does the fast rise time of the scintillation signal obtained with the xenon cell described previously. More investigation is required for the case of significant charge accumulation in the photocathode. This was not pursued for lack of a suitably fast source.

Dark current is also a concern in a detector such as ZEPLIN III, in which very small prompt scintillations must be identified in the history of a larger electroluminescence signal. PMT D730 #1 was stored in the dark for two weeks, and biased one day before cooling. At room temperature, ~ 20 counts/s were measured above 0.3 phe, which is almost one order of magnitude less than the value quoted by the manufacturer. Cooling to -100°C reduced the dark count rate by only 25%.

4. Discussion

The temperature coefficients found in our tests are in good agreement with those indicated by the manufacturer [8]: $-0.17\%/^{\circ}\text{C}$ is quoted for the QE in the blue, which is consistent with our observations at 175 nm, and $+0.05\%/^{\circ}\text{C}$ for green

wavelengths also agrees with our LED data. The value $-0.2\%/^{\circ}\text{C}$ quoted for the gain of CuBe dynodes is also consistent with our measurements.

Improved VUV response from cooling down to liquid xenon temperatures has been reported previously for different PMTs [4,5]. However, the biggest increase in overall response between room temperature and -100°C in our sample was 40%, which is much smaller than, for example, the 130% seen for a similar PMT (EMI 9750Q) in those previous studies. Several PMT models were tested in the same set-up, using two experimental techniques, and no explanation could be found for the markedly different behaviour seen for tubes from different manufacturers.

We propose that variations of photocathode thickness for different PMTs in our sample can explain some of the trends observed in the present study, namely, the different average photocurrents required to saturate the photocathodes (Fig. 7) and the distribution of changes in QE (Fig. 6).

The mean escape depth for photoelectrons decreases with energy below a few tens of eV in most solids (see, for example, Ref. [9]). As photocathode thicknesses are usually tuned to maximise response for visible light, higher-energy photoelectrons will have more difficulty escaping. Therefore, thinner (i.e. more resistive) photocathodes should provide better sensitivity to xenon scintillation (7 eV), which could explain why they also saturate more easily.

The diffusion of photoelectrons towards the photocathode surface is hindered by scattering with, among others, lattice phonons. This is one of the most temperature-sensitive process of the photoemission mechanism. The enhancement of the QE towards the blue part of the spectrum with cooling has long been attributed to a reduction in lattice scattering [10]. To estimate how such a decrease can affect photoemission, we consider a simple model for a photocathode of thickness t . Photons, entering from one side, are absorbed with attenuation length L . The photoelectrons thus produced can escape from the opposite side, with a probability which decreases exponentially away from the vacuum interface, characterised by a mean escape depth D , multiplied by an extraction efficiency η_{ex} . For an opaque layer ($L \ll t$),

which is a reasonable assumption for VUV photons, $QE(t) = \eta_{\text{ex}} \exp(-t/D)$ – i.e. thinner photocathodes have higher sensitivity. The variation $\Delta = (QE_1 - QE_0)/QE_0$, caused by a corresponding change in D , is given by:

$$\Delta = \left(\frac{QE_0}{\eta_{\text{ex}}} \right)^{D_0/D_1 - 1} - 1. \quad (1)$$

This equation predicts that photocathodes with higher QE improve less with an increase in D than poorer ones. A least squares fit to the data, also shown in Fig. 6, results in the parameters $\eta = 0.44 \pm 0.05$ and $D_1/D_0 = 1.22 \pm 0.05$. Although further experimental work is required to confirm this model, the values found for the extraction efficiency and increase in mean escape depth do appear sensible.

The relatively small decrease observed in dark current with cooling of the PMT can also be partly explained by this effect. Many dark counts are due to internal radioactivity and cosmic rays causing Cherenkov emission in the quartz window, and not many are thermally generated in the best bialkali photocathodes. Cooling reduces this thermionic component, but it also enhances photoelectron emission due to reduced scattering.

Concerning the signal saturation from accumulation of charge in the photocathode, it is apparent that the inclusion of metal fingers has not led to an increase in the maximum photocurrent allowed. Nevertheless, these metallisations do provide quicker recovery times from saturation: the discharge is several times faster in the D730 than in the parent PMT. An accurate analysis of this effect is not straightforward, owing to the complicated shape of the electric field at the photocathode. This is not only determined by the extraction field and the accumulated charge, but also by the metal fingers as well as by field penetration effects through the nearly-dielectric photocathode.

The background generated by PMT radioactivity is expected to dominate the overall count rate in the underground operation of ZEPLIN III. A figure of $\sim 100\,000$ γ -rays/day/PMT, resulting from our radioactivity measurements, can produce up to $\sim 2 \times 10^5$ phe/s in each tube. This value is

small compared to the saturation photocurrents given in Fig. 7. However, calibration with external radioactive sources can lead to far higher photon rates. A limit of 5×10^7 phe/s, low enough to prevent noticeable saturation at -100°C , sets a maximum energy deposition rate of the order of 350 MeV/s in the active region of the detector. This is considered sufficiently large to allow a speedy calibration.

5. Conclusions

We have described the test at low temperature of a set of 35 ETL D730 PMTs intended for use in the ZEPLIN III WIMP detector. The PMTs were shown to operate well at -100°C for average photocurrents of up to 10^8 phe/s. Most PMTs exhibited an increase in gain and in quantum efficiency at 175 nm with decreasing temperature, and recovered the initial room temperature performance after warming.

Cooling to liquid xenon temperatures produces an average 10% increase in QE at 175 nm. Individually, PMTs with lower QE at room temperature improve most when cooled. The changes in multiplication gain are less predictable from tube to tube, although a tendency is seen for improvement. Only three tubes had a decrease in their gain, and only one of these showed a simultaneous decrease in QE. Cooling did not affect very significantly the timing properties or the dark current.

Saturation of the photocathode response was observed for two D730 tubes (with metal fingers evaporated behind the photocathode) and found to occur at lower photon rates than for a similar PMT model without the metallisations. Notably, the tube with best QE in the sample saturated more easily than the one with worst QE.

Variations in photocathode thickness in the sample can account for these results. A simple model based on an increasing mean escape depth with decreasing temperature in photocathodes of different thicknesses has been proposed to explain the behaviour of the QE at 175 nm.

Acknowledgements

The authors wish to thank Electron Tubes Limited for their suggestions and their willingness to discuss the issues raised in this paper. Thanks are also due to D. Akimov (ITEP) for valuable comments on the manuscript. This work has been funded by the UK's Particle Physics And Astronomy Research Council (PPARC).

References

- [1] T.J. Sumner, in: N.J.C. Spooner, V. Kudryavtsev (Eds.), Proceedings of the 3rd International Workshop on the Identification of Dark Matter, World Scientific, Singapore, 2001, p. 452.
- [2] J.E. McMillan, R.J.O. Reid, *J. Phys. E* 22 (1989) 377.
- [3] M. Ichige, et al., *Nucl. Instr. and Meth. A* 327 (1993) 144.
- [4] H.M. Araújo, et al., *Rev. Sci. Instrum.* 68 (1) (1997) 34.
- [5] H.M. Araújo, et al., *IEEE Trans. Nucl. Sci.* NS-45 (3) (1998) 542.
- [6] Electron Tubes Ltd, UK www.electrontubes.com.
- [7] A.S. Howard, et al., in: N.J.C. Spooner, V. Kudryavtsev (Eds.), Proceedings of the 3rd International Workshop on the Identification of Dark Matter, World Scientific, Singapore, 2001, p. 457.
- [8] ETL brochure, Understanding Photomultipliers, ref upmt/01, 2001
- [9] S. Hüfner, *Photoelectron Spectroscopy*, 3rd Edition, Springer, Berlin, 2003.
- [10] W.E. Spicer, F. Wooten, *Proc. IEEE* 51 (1963) 1119.